



Rational Designed Polymer as a Metal-Free Catalyst for Hydroxylation of Benzene to Phenol with Dioxygen

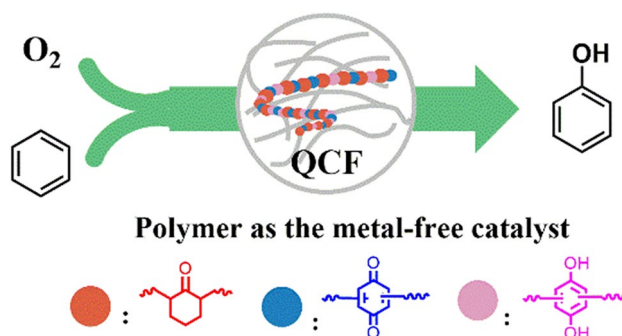
Weitao Wang¹ · Yaoyao Wei¹ · Xulu Jiang¹ · Zhen-Hong He¹ · Cunshe Zhang² · Zhao-Tie Liu^{1,3}

Received: 23 July 2020 / Accepted: 4 September 2020
© Springer Science+Business Media, LLC, part of Springer Nature 2020

Abstract

Direct hydroxylation of benzene to phenol with dioxygen is a green route for synthesis of phenol. The higher bonding energies of C–H in benzene and O–O in dioxygen make metal-free catalysis a challenge. A novel metal-free catalyst of quinone-cylcohexanone-formaldehyde polymer was rationally designed and prepared. The polymer was characterized with FT-IR, XRD, Raman, SEM, ¹³C NMR and XPS. Abundant oxygen functional groups of cyclic ketonic, quinone carbonyl and hydroquinone were found on the surface of polymer. The catalytic performances for hydroxylation of benzene to phenol with dioxygen over the metal-free catalyst were investigated and a phenol yielding of 11.4% was achieved. Moreover, the reaction mechanism was proposed.

Graphic Abstract



Keywords Green chemistry · Catalysis · Aerobic oxidation · Liquid-phase oxidation · Partial oxidation · Hydroxylation · Benzene · Metal-free catalysis

Electronic supplementary material The online version of this article (<https://doi.org/10.1007/s10562-020-03392-9>) contains supplementary material, which is available to authorized users.

✉ Weitao Wang
wangweitao@sust.edu.cn

✉ Zhao-Tie Liu
ztliu@snnu.edu.cn

¹ Shaanxi Key Laboratory of Chemical Additives for Industry, College of Chemistry & Chemical Engineering, Shaanxi University of Science & Technology, Xi'an, Shaanxi 710021, China

² Shaanxi Key Laboratory of Petroleum Fine Chemicals, Shaanxi Provincial Research and Design Institute of Petroleum and Chemical Industry, Xi'an, Shaanxi 710054, China

³ School of Chemistry & Chemical Engineering, Shaanxi Normal University, Xi'an, Shaanxi 710119, China

2 Experimental

2.1 Materials

All reagents were commercially available and used without additional purification. Benzene was obtained from Shanghai Macklin Biochemical Co., Ltd. *p*-Benzoquinone and acetic acid were obtained from Sinopharm Chemical Reagent CO., Ltd. Formaldehyde solution and cyclohexanone were purchased from Shanghai Aladdin Reagent CO., Ltd.

2.2 Catalyst Preparation

The QCF was synthesized by a one-step solvothermal method (Fig. S1). Typically, 8.0 mmol *p*-benzoquinone, 8.0 mmol cyclohexanone, and 1.8 g 37% formaldehyde aqueous solution were mixed in 20 mL ethyl alcohol, then the mixture was stirred for 20 min at 65 °C. Subsequently, 200 μ L 30% sodium hydroxide solution was added in the mixture. The mixture was raised to 85 °C and stirred for 10 min. After that, the mixture was transferred into a Teflon-lined autoclave and heated at 200 °C for 5 h. The product was separated by filtration, washed with ethanol and dried at 80 °C. The obtained powder was denoted as QCF-*n*, in which *n* represents the molar ratio of quinone to ketone.

2.3 Characterization

XRD (X-ray diffraction) patterns were obtained by using Cu K α radiation, nickel filter, 40 kV/40 mA, scanning mode of 2 theta/theta, scanning type of continuous scanning, and a scanning range from 3° to 90° at a scanning rate of 8°/min (Ultima IV, Rigaku). XPS (X-ray photoelectron spectroscopy) spectra (Axis Ultra, Kratos Analytical Ltd.) were using 300 W Al K α radiation with the binding energies calibrated at 284.6 eV from C1s of the adventitious carbon. Asymmetrical XPS peaks were deconvoluted by using the curve-fitting approach with CasaXPS software, as well as by applying Shirley background subtraction and Lorentzian–Gaussian functions (30%G). Surface area of the catalysts was conducted by the adsorption of N₂ at –196 °C, the catalyst sample was degassed in vacuum at 150 °C for 10 h before N₂ adsorption (Gemini VII 2.00, Micromeritics Instrument Corporation). Raman spectra were recorded on a LabRam-1B microscopic Raman spectrometer with 532 nm laser excitation. Fourier transform infrared spectroscopy (FT-IR) was performed on a VECTOR-22 using the KBr pellet technique with a resolution of 2 cm^{–1} from 400 to 4000 cm^{–1} and consisted of 32 scans

at room temperature. Scanning electron microscope (SEM) for the sample morphology was measured at 20 kV and 15 mA on the Hitachi S-4800. The solid state ¹³C NMR was conducted on the Agilent 600 M.

2.4 Benzene Hydroxylation Reaction

Aerobic hydroxylation of benzene to phenol was carried out in a high-pressure seal reactor. In a typical run, 0.5 mL (5.62 mmol) of benzene, 0.1 g of QCF, 0.4 g of LiOAc, and 3.0 mL 70%(V/V) acetic acid aqueous solution were added into the reactor successively. After the reactor was charged with 3.0 MPa O₂ at room temperature, the reaction was conducted at 140 °C for 12 h with vigorous stirring. After the reaction, the catalyst was separated by centrifugation. The solution was diluted to 50 mL in a volumetric flask with methanol. Concentrations of phenol in the solution were measured by high performance liquid chromatography (HPLC, WAYEE LC 3000–2 Series instrument) using an Ultimate MBC18 (250 mm \times 4.60 mm) column by UV detector at 254 nm wavelength. The temperature of column is 40 °C. The mobile phase consisted of a methanol/water solution 30/70 (V/V) fed at a flow-rate of 1.0 mL/min. The CO₂ and some undefined compounds were detected in the products (Fig. S2, Fig. S3). The yield of phenol was calculated with the external standard method according to the formula:

$$\text{Yield of phenol} = \frac{\text{mmol of phenol}}{\text{mmol of initial benzene}} \times 100$$

3 Results and Discussion

The functional groups of the QCF were characterized by the FT-IR (Fig. S4a). All the resins showed a similar IR spectra. The peaks at 3300–3600 cm^{–1} were attributed to the vibration of –OH. The peaks at ~2923 cm^{–1} and ~2858 cm^{–1} were assigned to the C–H vibration in –CH₂– and –CH–. The peaks at about 1790, 1709, and 1652 cm^{–1} were contributed by C=O in aldehyde, ketone, and quinone [20], respectively. With the molar ratio of quinone to ketone increased, the intensity of quinone group peak relatively increased, indicating the content of quinone groups in the QCF increased. The peak at 1447 cm^{–1} was assigned to the $\sigma_{\text{C-H}}$ of methylene linker while peaks at 1380 cm^{–1} and 1330 cm^{–1} were attributed to the $\sigma_{\text{C-H}}$ of aromatic ring [20, 21]. The 1583 cm^{–1} and 1250 cm^{–1} can be assigned to the $\nu_{\text{C=C}}$ in aromatic ring and $\nu_{\text{C-O}}$ in hydroquinone [22], suggesting the existence of hydroquinone groups in the QCFs. The X-diffraction patterns exhibited broad peaks for the QCFs, indicated that QCFs were amorphous (Fig. S4b). Two peaks can be found

in the Raman spectra of the QCFs (Fig. S4c). The broad peak at $\sim 1353\text{ cm}^{-1}$ was attributed to the D mode related to the sp^3 -hybridized carbon. The peak at $\sim 1585\text{ cm}^{-1}$ in the Raman spectra was attributed to G peak related to the sp^2 -hybridized carbon [23]. The I_D/I_G can be employed to indicate the relatively content of sp^3 - and sp^2 - carbon. It can be found that the content of sp^3 -hybridized carbon in QCF decreased with an increase of the molar ratio of quinone to ketone. N_2 adsorption–desorption analysis of the QCFs (Fig. S4d) revealed a typical type III isotherm. The BET surface areas were 8.6, 8.4, $13.6\text{ m}^2\cdot\text{g}^{-1}$ for QCF-0.5, QCF-1, and QCF-2, respectively. This indicated that the molar ratio of quinone to ketone affected the texture structure of the resins by the polymerization structures. The solid ^{13}C NMR was characterized to verified the structure of the QCF (Fig. S5). The peak at about 27 ppm revealed the existence of $-\text{CH}_2-$ in the linker and cyclohexanone groups. The peaks at about 48 ppm and 79 ppm corresponded to the $-\text{CH}-$ and $-\text{CH}_2-\text{OH}$. The peaks at about 122 ppm and 146 ppm were attributed to the carbon in benzene and phenolic hydroxyl, respectively. The $\text{C}=\text{O}$ in quinone and ketone were found at about 186 ppm and 214 ppm. The solid ^{13}C NMR spectrum verified the structure of QCF in Scheme 1. The images of SEM shows the QCF was in the form of spherical particles (Fig. S6).

XPS revealed that three peaks of carbon in QCFs (Fig. 1a). The peaks of C1s at 284.6, 286.1, and 288.6 eV were assigned to the aromatic/aliphatic carbon, C–OH, and $\text{C}=\text{O}$ [5], respectively. Two kinds of oxygen species were found on the surface of the QCFs (Fig. 1b), in which the binding energy of O1s at 531.8 eV was attributed to $\text{C}=\text{O}$ while the peak at 533.8 eV was the C–OH [19]. The surface oxygen content increased from 19.0 to 20.2 at.% with the increase of molar ratio of quinone to ketone from 0.5 to 1. But the oxygen content decreased to 17.4 at.% when the molar ratio increased to 2. From the above characterization, it can be confirmed that the existence of the groups of quinone, phenolic hydroxyl, ketone, and CH_2 linker. Therefore, the QCF structure was deduced as Scheme 1.

Table 1 Hydroxylation of benzene to phenol over QCF

Entry	Catalyst	Solvent	Temperature ($^{\circ}\text{C}$)	Yield (%)
1	QCF-1	Acetonitrile	140	trace
2	QCF-1	Ethanol	140	trace
3	QCF-1	DMF	140	trace
4	QCF-1	DMSO	140	trace
5	QCF-1	Acetic acid (70%)	140	10.4
6	QCF-1	Acetic acid (70%)	120	2.8
7	QCF-1	Acetic acid (70%)	130	6.9
8	QCF-1	Acetic acid (70%)	150	6.1
9	QCF-0.5	Acetic acid (70%)	140	6.1
10	QCF-2	Acetic acid (70%)	140	3.3
11	QCF-carbon ^a	Acetic acid (70%)	140	trace

Catalytic reaction conditions: benzene (0.5 mL), catalyst (100 mg), solvent (3.0 mL), LiOAc (0.4 g), O_2 (3.0 MPa); 12 h

^aQCF was calcined at $900\text{ }^{\circ}\text{C}$ under nitrogen atmosphere

The prepared QCF was employed as the catalyst for the hydroxylation of benzene to phenol. The reaction solvent was screened (Table 1). It was found that no phenol was yielded in the solvents of acetonitrile, ethanol, DMF, and DMSO. It can yield 10.4% phenol in the solvent of acetic acid aqueous solution. This indicated that the acid proton solvent was important for the QCF catalytic system. The reaction temperature was examined from $120\text{ }^{\circ}\text{C}$ to $150\text{ }^{\circ}\text{C}$. The yield of phenol increased firstly, and then decreased with the increase of temperature, giving a maximum yield at $140\text{ }^{\circ}\text{C}$. This was consistent with the reaction temperature range of $120\text{ }^{\circ}\text{C}$ to $150\text{ }^{\circ}\text{C}$ for the reductant-free metal-based catalytic reaction system [19]. As expected, the loading of the QCF affected the catalytic performance. With the increase of the QCF loading, the yield of phenol increased first, and then declined (Table S1). The yield of phenol increased with the increase of oxygen pressure and reached the platform under the pressure of 3.0 MPa (Table S2). The amount of LiOAc additive affected the reaction. The optimized amount

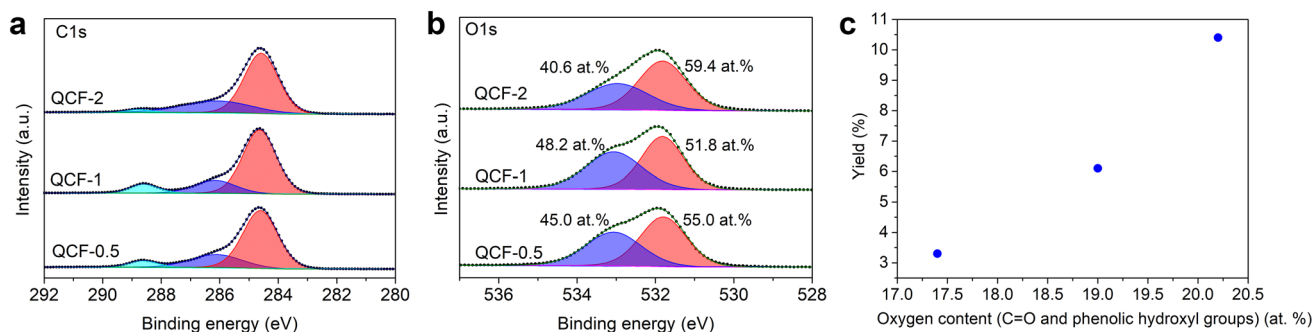


Fig. 1 The XPS spectra of **a** C1s and **b** O1s in QCFs. **c** Relationship between the phenol yield and the surface oxygen content of QCF

of LiOAc additive was 0.4 g (Table S3). With the increase of the reaction time, the yield of phenol increased and reached 11.4% at 24 h (Table S4). The yield of phenol with QCF-1 as catalyst reached catalytic performance level of the metal-based catalyst (Table S5). The QCF-2 and QCF-0.5 showed lower yield of phenol than that of QCF-1, implying that the group content in the QCF affected the reaction activity. The relationship between the oxygen content (C=O and phenolic hydroxyl groups) and the yield of phenol was roughly linear (Fig. 1c), indicating the surface oxygen functional groups are active sites. This was further confirmed by that there was no phenol detected when the oxygen groups of the QCF were removed by calcination of QCF at 900 °C under nitrogen atmosphere (Table 1, entry 11).

The phenol could not be yielded without the QCF catalyst, suggesting that the QCF provided the active sites for the hydroxylation of benzene to phenol (Table 2). In absence of the LiOAc additive, the yield of phenol decreased from 10.4% to 7.3%. With LiCl as the additive, trace phenol was found, indicating that the Li⁺ ion was not the main effective content in the additive. This was due to the enthalpy of the formation of Li⁺(Ben) and Li⁺(phenol) was nearly equal [24, 25] (Table S6), indicating the interaction between Li⁺ ion and benzene or phenol was equal. In addition, the yield of phenol varied little when NaOAc additive was added in the catalytic system instead of LiOAc. Therefore, it can be deduced that the OAc⁻ was the effective content provided by the additives. The acetated salts can form the buffer solution with the acetic acid aqueous solution to give the acidic

Table 2 The controlled experiments for hydroxylation of benzene to phenol

Entry	Conditions	Yield (%)
1	No catalyst	— ^a
2	No LiOAc	7.3
3	Standard condition	10.4
4	LiCl ^b	trace
5	NaOAc ^b	10.7
6	BHT (5.7 mmol)	0.5
7	BHT (8.5 mmol)	0.4
8	<i>t</i> -Butanol (5.7 mmol)	5.9
9	<i>t</i> -Butanol (8.5 mmol)	2.9
10	No O ₂	— ^{ac}
11	H ₂ O ₂	3.7 ^d

Catalytic reaction conditions: benzene (0.5 mL), catalyst (100 mg), 70%(V/V) acetic acid (3.0 mL), LiOAc (0.4 g), O₂ (3.0 MPa), 12 h

^aNo phenol was detected

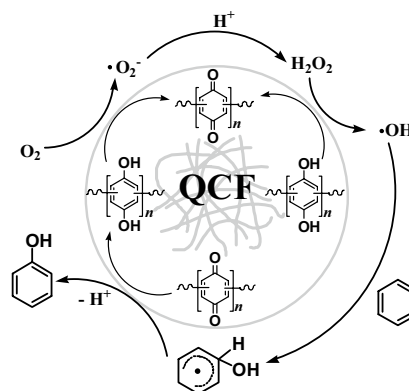
^bEquivalent LiCl or NaOAc was added instead of LiOAc

^cThe reaction was carried out under N₂ atmosphere

^dThe reaction was carried out with H₂O₂ (30 wt.%, 1.0 mL) as the oxidant under N₂ atmosphere.

reaction environment [11]. When the radical scavengers of the *t*-butanol (•OH radical scavenger) and BHT (butylated hydroxytoluene, •O₂⁻ radical scavenger) were added in the reaction system, the yield of phenol reduced to 2.9% and 0.4%, respectively, indicating that both hydroxyl radical (•OH) and superoxide radical (•O₂⁻) were involved in the reaction. To test whether the oxygen activation was involved in the initial step in the aerobic oxidation reaction, the reaction was carried out under molecular oxygen-free condition (Table 2, entry 10). The yield of phenol was not detected, excluding the involving of surface oxygen species over the QCF in the initial step of reaction but indicating that the oxygen molecule activation was involved in the initial step.

From the findings of the controlled experiments, it can be demonstrated that (1) the active sites were the surface oxygen species, (2) hydroxyl radical and superoxide radical were involved in the reaction, (3) O₂ activation was involved in the initial step. Based these, the possible reaction route was proposed for the present hydroxylation of benzene to phenol (Scheme 2). The O₂ was chemisorbed on the surface oxygen functional groups (ketonic/quinone C=O, and hydroquinone) and then was activated to generate •O₂⁻ [18]. At the acidic environment, •O₂⁻ can combine H⁺ to form HO₂•. Subsequently, two HO₂• radicals easily combine to form H₂O₂ and O₂. Because rate constant of combination reaction of HO₂• radicals is larger than that of the reaction for HO₂• radicals attacking benzene [19, 26]. Therefore, H₂O₂ was generated by two HO₂• radicals. •OH was generated from H₂O₂ on the surface of the QCF. It is the •OH radical that attacked the benzene ring to form phenol due to the reaction rate for •O₂⁻ and HO₂• attacking benzene is much lower than that of •OH [26]. From this reaction route, it can explain why the hydroxyl radical (•OH) and superoxide radical (•O₂⁻) scavengers can greatly decrease the yield of phenol. Moreover, this was proved by the yield of 3.7% phenol with the H₂O₂ as the oxidant without O₂



Scheme 2 Proposed reaction pathway for hydroxylation of benzene to phenol over QCF

(Table 2, entry 11), but no phenol was yielded without O₂ (Table 2, entry 10).

4 Conclusion

In summary, we have developed a novel quinone-cyclohexanone-formaldehyde polymer as a metal-free catalyst for hydroxylation of benzene to phenol with dioxygen. The polymer was characterized to possess the oxygen functional groups of quinone, phenolic hydroxyl, and ketone. The oxygen groups were the active sites for the reaction. Under the optimized reaction condition, 11.4% phenol can be obtained. This catalyst confirmed the idea that rationally designed catalyst with the oxygen groups of quinone, phenolic hydroxyl, and ketone can be employed to catalyze the hydroxylation reaction. This provides a promising candidate for designing the metal-free catalyst for the hydroxylation of benzene to phenol.

Acknowledgements The authors gratefully acknowledge the financial supports from the National Natural Science Foundation of China (No. 21403136, 21978160), Natural Science Basic Research Plan in Shaanxi Province of China (No. 2019JM-080, 2019JLM-16, 2019ZDLGY06-04), and Foundation of Chemical Industry Shaanxi Key Laboratory of Petroleum Fine Chemicals.

Compliance with Ethical Standards

Conflict of interest There is no conflict of interest for each contributing author.

References

- Zhou Y, Ma Z, Tang J, Yan N, Du Y, Xi X, Wang K, Zhang W, Wen H, Wang J (2018) *Nat Commun* 9:2931
- Jiang T, Wang W, Han B (2013) *New J Chem* 37:1654–1664
- Lücke B, Narayana KV, Martin A, Jähnisch K (2004) *Adv Synth Catal* 8:1407–1424
- Huang Y-L, Pellegrinelli C, Wachsman ED (2017) *ACS Catal* 7:5766–5772
- Wang W, Shi L, Li N, Ma Y (2017) *RSC Adv* 7:12738–12744
- Long Z, Chen G, Liu S, Huang F, Sun L, Qin Z, Wang Q, Zhou Y, Wang J (2018) *Chem Eng J* 334:873–881
- Shang S, Chen B, Wang L, Dai W, Zhang Y, Gao S (2015) *RSC Adv* 5:31965–31971
- Okamura J, Nishiyama S, Tsuruya S, Masai M (1998) *J Mol Catal A: Chem* 135:133–142
- Okemoto A, Ueyama K, Taniya K, Ichihashi Y, Nishiyama S (2017) *Catal Commun* 100:29–32
- Shang S, Hua Y, Li J, Bo C, Ying L, Shuang G (2014) *ChemPlusChem* 79:680–683
- Qin Q, Liu Y, Shan W, Hou W, Wang K, Ling X, Zhou Y, Wang J (2017) *Ind Eng Chem Res* 56:12289–12296
- Long Z, Zhou Y, Chen G, Ge W, Wang J (2014) *Sci Rep* 4:3651–3651
- Liu Y, Murata K, Inaba M (2006) *J Mol Catal A: Chem* 256:247–255
- Wang W, Yao M, Ma Y, Zhang J (2014) *Prog Chem* 26:1665–1672
- Li Y, Li B, Chen T, Zhou Z, Wang J, Huang J (2015) *Chinese J Catal* 36:1086–1092
- Wang W, Li N, Tang H, Ma Y, Yang X (2018) *Mol Catal* 453:113–120
- Zhu J, Li G, Wang Q, Zhou Y, Wang J (2019) *Ind Eng Chem Res* 58:20226–20235
- Shan W, Li S, Cai X, Zhu J, Zhou Y, Wang J (2019) *Chem-CatChem* 11:1076–1085
- Wang W, Tang H, Jiang X, Huang F-E, Ma Y (2019) *Chem Commun* 55:7772–7775
- Shiraishi Y, Takii T, Hagi T, Mori S, Kofuji Y, Kitagawa Y, Tanaka S, Ichikawa S, Hirai T (2019) *Nat Mater* 18:985
- Yang G, Jiang J, Zhang Y (2015) *Prog Org Coat* 78:55–58
- Poljanšek I, Krajnc M (2005) *Acta Chim Slov* 52:238–244
- Ou J, Wang J, Liu S, Mu B, Ren J, Wang H, Yang S (2010) *Langmuir* 26:15830–15836
- Feller D, Dixon DA, Nicholas JB (2000) *J Phys Chem A* 104:11414–11419
- Zierkiewicz W, Michalska D, Černý J, Hobza P (2006) *Mol Phys* 104(13–14):2317–2325
- Vysotskaya NA (1973) *Russ Chem Rev* 42:851–856

Publisher's Note Springer Nature remains neutral with regard to jurisdictional claims in published maps and institutional affiliations.